IEEE Access
Multidisciplinary ⋮ Rapid Review ⋮ Open Access Journal

Received 24 March 2024, accepted 11 April 2024, date of publication 23 April 2024, date of current version 3 May 2024.

*Digital Object Identifier 10.1109/ACCESS.2024.3392767*

RESEARCH ARTICLE

# Investigating the Impact of Electrical Load Types on the Frequency Response of Low Inertia Power Systems

**MAHYAR TOFIGHI-MILANI**[1], **SAJJAD FATTAHEIAN-DEHKORDI**[1,2], **(Graduate Student Member, IEEE), AND MATTI LEHTONEN**[1]

[1]Department of Electrical Engineering and Automation, Aalto University, 02150 Espoo, Finland
[2]Institute of Energy Systems, Energy Efficiency and Energy Economic, TU Dortmund University, 44227 Dortmund, Germany

Corresponding author: Sajjad Fattaheian-Dehkordi (sajjad.fattaheiandehkordi@aalto.fi)

**ABSTRACT** In the contemporary power system landscape, characterized by a significant integration of renewable resources and the proliferation of inverter-connected devices, system inertia is on a declining trajectory. In this evolving scenario, the influence of various load types on system frequency becomes significant. In this regard, it seems that a comprehensive study on the effect of load types on the system's frequency is missing in the literature. Hence, this paper aims to fill this gap by aggregating various load models known to affect system frequency and subsequently assessing the influence of each load type on the power systems' frequency response. To achieve this, the IEEE 30-bus test system is employed to investigate the impact of different load parameters and their penetration levels on the systems' frequency response.

**INDEX TERMS** Dynamic load models, frequency-dependent models, frequency response, load modeling, static load models, time delayed loads.

## NOMENCLATURE

### *ABBREVIATIONS*

| | |
|---|---|
| *IM* | Induction motor. |
| *NPD* | Nadir point deviation. |
| *NT* | Nadir time. |
| *PL* | Penetration level. |
| *RoCoF* | Rate of change of frequency. |
| *SFD* | Settling frequency deviation. |
| *ST* | Settling time. |
| *TD* | Time-delayed loads. |
| *TDI* | Time-delayed load model (type one). |
| *TDII* | Time-delayed load model (type two). |
| *ZC*, *IC*, *PC* | Impedance-, current-, and power-constant load models. |
| *ZIP*, *EXP* | ZIP and exponential load model. |

### *PARAMETERS*

| | |
|---|---|
| $\Delta f$, $\Delta t$ | Frequency and time increment. |
| $\Delta P_{TDI}$, $\Delta P_{TDII}$ | The power increment amount of TDI and TDII load. |
| $\omega$ | The angular speed of reference frame. |
| $\omega_m$ | The angular speed of the rotor. |
| $\omega_r$ | Electrical angular speed. |
| $\phi'_{dr}$, $\phi'_{qr}$ | Rotor's d-axis and q-axis fluxes. |
| $\phi_{ds}$, $\phi_{qs}$ | Stator's d-axis and q-axis fluxes. |
| $\theta_m$ | The angular position of the rotor. |
| $F$ | The viscous friction coefficient of the rotor and load. |
| $H$ | Inertia of the induction motor. |
| $k_{TDI}$, $k_{TDII}$ | Largeness parameter of TDI and TDII models. |
| $k_{ZIP}$, $k_{EXP}$ | The parameters of ZIP and EXP models. |
| $L_m$ | Magnetizing inductance. |
| $L'_r$ | Total inductance of rotor. |
| $L_s$ | Total inductance of stator. |
| $p$ | Number of pole pairs. |

The associate editor coordinating the review of this manuscript and approving it for publication was Fabio Mottola.

| | |
|---|---|
| $P_n, V_n, f_n$ | Nominal power, voltage, and frequency. |
| $P_{ZIP}, P_{EXP}$ | The power amount of the ZIP and EXP load. |
| $R_r^{'}, L_{lr}^{'}$ | The resistance and leakage inductance of rotor. |
| $R_s, L_{ls}$ | The resistance and leakage inductance of stator. |
| $T_e$ | Electromagnetic torque. |
| $T_m$ | The mechanical torque of the shaft. |
| $t_{TDII}, \tau_{TDII}$ | Delay time and time constant of TDII models. |
| $t_{TDI}, \tau_{TDI}$ | Delay time and time constant of TDI models. |
| $V, f$ | Voltage and frequency. |
| $V_{dr}^{'}, i_{dr}^{'}$ | The d-axis voltage and current of rotor. |
| $V_{ds}, i_{ds}$ | The d-axis voltage and current of stator. |
| $V_{qr}^{'}, i_{qr}^{'}$ | The q-axis voltage and current of rotor. |
| $V_{qs}, i_{qs}$ | The q-axis voltage and current of stator. |

## I. INTRODUCTION

In order to deliver quality and sustainable power to electrical loads, the frequency of electricity should be maintained within a certain range, close enough to the nominal value. In general, frequency deviations in power systems result from imbalances between power generation and consumption, and they are adjusted by means of generators' governor action through primary frequency control (PFC). The PFC process typically stabilizes the frequency of the system within less than 30 seconds. Nonetheless, in modern power systems, there is doubt about the capability of this method to regulate the system frequency, especially with the undisputed high penetration of intermittent renewable resources [1], [2]. Moreover, the increasing implementation of inverter-connected distributed energy resources decreases the power system's inertia, which leads to higher deviations of the system's frequency [3].

Considering these changes, in future power systems, the effect of electrical loads will be significant on the frequency response of the power system [4]. Understanding this impact allows operators to estimate the contribution of each load type on the frequency response of the system. This understanding is valuable especially in isolated power grids with high renewable energy penetration, such as Cyprus's grid [5]. In this regard, in spite of the recognition and declaration of the need for precise load modeling by researchers [6], it seems that further research is required for a better understanding of load characteristics [7].

The aim of load modeling is to create straightforward mathematical representations to estimate load behaviors [7]. Various load models have been proposed in the literature, which could be divided into two major load groups: static loads and dynamic loads. In static loads, there is a mathematical relationship between the power consumption amount of the load and the voltage as well as the frequency of the bus to which the load is connected. However, dynamic load models include the time dependence, in addition to the voltage and frequency, to describe the system loads' dynamic behavior [8].

The most well-known models that have been considered in the literature for static loads are the ZIP and exponential (EXP) models [9]. In the ZIP load, the power is modeled as a polynomial equation, while in the EXP load, it is modeled by an exponential function of voltage and frequency. It is noteworthy that ZIP loads can be specialized and converted to impedance-constant (ZC), current-constant (IC), and power-constant (PC) load models as static loads.

Many research works have been done around static load modeling. For example, authors of [3] use the ZIP and EXP load models to investigate the impact of load composition on transient stability in a medium voltage microgrid in case of islanding transitions. Additionally, they emphasize the significance of accurate load modeling for analyzing the microgrid's transient response during islanding. Reference [10] specifically investigates how numerical models of passive components in power systems, such as lines, transformers, and on-load tap changers, affect stability analyses. To this end, this paper uses the ZC and PC load models in its simulations. Reference [11] presents a framework for assessing the integration of renewables into the power system while ensuring stable frequency performance by analyzing various scenarios and parameters, taking a ZIP model into account.

In the context of research concerning static loads, several studies (e.g., [10], [12], [13]) have employed either the ZC, IC, or PC models individually or in combination. Additionally, certain papers have focused solely on the ZIP model (such as references [11], [14], [15], [16], [17], and [18]) or the EXP model (e.g., [5], [19]). Notably, a group of authors (such as those in references [20], [21], [22], [23], [24], and [25]) has taken both ZIP and EXP load models in their investigations, simultaneously. However, none of the mentioned references (i.e., [5], [10], [11], [12], [13], [14], [15], [16], [17], [18], [19], [20], [21], [22], [23], [24], [25]) have explored the system's frequency response with specifically examining the effects of ZIP or EXP load models.

In addition to static load models, dynamic models are essential in power systems. Static models alone are insufficient as they neglect time dependency, making them unable to accurately represent all electrical loads in the system. In this context, the most widely recognized dynamic load in power systems is the induction motor (IM) [9]. Many researchers have attempted to study IMs with the aim of recognizing/modeling their behavior/effect in power systems. For instance, reference [26] introduces a straightforward IM model for system frequency response simulations. This paper also demonstrates the agreement between the responses of this proposed IM model and a more complex nonlinear IM model. Meanwhile, in the study of reference [27], the authors aim to understand how IMs affect grid inertia. To do this, they introduce two model types: a detailed grid model and a dynamic equivalent model that accounts for multiple

induction motors. Additionally, several other references (such as [5], [12], [13], [14], [15], [17], [18], [19], [20], [22], [23], [24], [25], and [27]) have explored IMs from various perspectives. However, they did not directly investigate the impact of IM inertia on the system's frequency response.

In the realm of frequency analysis, reference [8] aims to explore the impact of ZIP and EXP models on system frequency, while reference [3] delves into the influence of the EXP model on the frequency response's nadir point. Authors of [26] have surveyed the effect of IMs' inertia on frequency response. However, these studies lack a comprehensive examination of all frequency response metrics, such as settling frequency deviation, rate of change of frequency (ROCOF), nadir point deviation, settling time, and nadir time, which leaves gaps in the overall analysis.

Therefore, it seems that a comprehensive frequency study, in which the impact of all load models is investigated in the various metrics of frequency response, is lacking in the literature. In this regard, the aim of this study is to probe the effect of various parameters of ZIP, EXP, and IM load models, as well as their penetration level, on the system's frequency response metrics (i.e., settling frequency deviation, RoCoF, nadir point deviation, settling time, and nadir time). Also, the impact of various mechanical load types that could be connected to IMs on the frequency response of the system is investigated in terms of the mentioned metrics in this paper.

Furthermore, this paper proposes a comprehensive time-delayed (TD) load model building upon the simplistic TD model proposed by [4]. TD loads represent a category of dynamic loads characterized by delayed responses. It is noteworthy that reference [4] examines the effect of a basic TD model on frequency response settling time. However, in this paper, we investigate the impact of the proposed TD model, alongside the previously established simple TD model, on system frequency response across all aforementioned frequency metrics. Hence, the contribution of this work could be summarized in the following points.

- Developing a comprehensive TD load model
- Exploring a thorough analysis of the impact of ZIP, EXP, IM, and TD load models as well as the effects of various IM mechanical load types on frequency response
- Conducting an investigation of load frequency response and comparing the results for each load type, considering nadir point, settling time, frequency deviation, and RoCoF

It is noteworthy that the reviewed papers in literature have all been classified in terms of the aforementioned static and dynamic load types (i.e., ZIP, EXP, IM, and TD) in Table 1. Additionally, research studies in the realm of load modeling could be categorized into three general groups of small signal, frequency, and voltage studies. Therefore, the reviewed papers have been classified also in Table 1. from this perspective.

The rest of the paper is organized as follows. Section II delves into load models, initially focusing on static loads, categorizing them, and subsequently transitioning to the study of dynamic load models. Moving on to Section III, the key metrics used to evaluate the frequency response of the system are introduced and defined. Section IV comprises three distinct studies. The first investigates the influence of diverse load parameters on system frequency response. The second study delves into the impact of varying load penetration levels on frequency. Lastly, the effects of different mechanical load types are explored when connected to IMs.

**TABLE 1. Taxonomy of reviewed papers according to study types and load types.**

| Refs | Load type | | Study type | | |
|---|---|---|---|---|---|
| | Static load consideration | Dynamic load consideration | Small signal | Frequency | Voltage |
| [16] | ZIP | - | - | - | - |
| [17], [18] | ZIP | IM | - | - | ✓ |
| [14] | ZIP | IM | ✓ | - | ✓ |
| [26] | - | IM | - | ✓ | ✓ |
| [19] | EXP | IM | - | ✓ | ✓ |
| [3], [20], [22] | ZIP, EXP | IM | - | ✓ | ✓ |
| [21] | ZIP, EXP | - | - | ✓ | ✓ |
| [13] | ZC, EXP | IM | - | ✓ | ✓ |
| [27] | - | IM | ✓ | ✓ | - |
| [23] | ZIP, EXP | IM | ✓ | ✓ | - |
| [10] | ZC, PC | - | ✓ | ✓ | ✓ |
| [8] | ZIP, EXP | - | ✓ | ✓ | ✓ |
| [24] | ZIP, EXP | IM | ✓ | ✓ | ✓ |
| [28], [29] | - | - | - | ✓ | - |
| [11] | ZIP | - | - | ✓ | - |
| [4] | - | TD | - | ✓ | - |
| [5] | EXP | IM | - | ✓ | - |
| [25] | ZIP, EXP | IM | - | ✓ | - |
| [15] | ZIP | IM | - | ✓ | - |
| [12] | ZC, IC | IM | - | ✓ | - |
| This paper | ZIP, EXP | IM, TD | - | ✓ | - |

## II. LOAD MODELING

In this section, the models used or devised in this paper are represented. Without loss of generality, all electrical loads can be divided into two general groups of static and dynamic load. By definition, a static load model describes the load properties at any moment of time as a mathematical function of bus voltage and/or bus frequency. Nevertheless, there are some loads that do not respond immediately to the voltage and frequency changes so that the dynamics of load components should be taken into account [6]. Therefore, in addition to the voltage and frequency, dynamic load models include the time dependence to model the dynamic behavior of the load [8]. In the rest of this section, first, the static load models considered in this paper is defined and illustrated, and then the considered dynamic load models are explained.

### A. STATIC LOAD MODELS

Static loads respond rapidly to system changes and are typically modeled as functions of instantaneous voltage or frequency. In research, these loads are frequently represented using ZIP and EXP models, with varying focus on voltage

**TABLE 2. Static load models classification.**

| Refs | Mathematical terms of load models | | | | | |
|---|---|---|---|---|---|---|
| | EV | ZC | IC | PC | LF | EF |
| [30] | ✓ | - | - | - | - | - |
| [13] | ✓ | ✓ | - | - | - | - |
| [12] | - | ✓ | ✓ | - | - | - |
| [10] | - | ✓ | - | ✓ | - | - |
| [14], [16], [18] | - | ✓ | ✓ | ✓ | - | - |
| [20], [22], [24] | ✓ | ✓ | ✓ | ✓ | - | - |
| [23], [25] | ✓ | ✓ | ✓ | ✓ | - | ✓ |
| [5], [19] | ✓ | - | - | - | ✓ | - |
| [3], [21] | ✓ | ✓ | ✓ | ✓ | ✓ | - |
| [17] | ✓ | - | - | ✓ | ✓ | - |
| [15] | - | ✓ | ✓ | ✓ | ✓ | - |
| [8] | ✓ | ✓ | ✓ | ✓ | ✓ | ✓ |
| This paper | - | - | - | ✓ | ✓ | ✓ |

or frequency aspects. In the literature, papers have used one, two, or several of the mathematical terms $P_n(\frac{V}{V_n})^2$, $P_n(\frac{V}{V_n})$, $P_n$, $P_n(1+k_f\Delta f)$, $P_n(\frac{V}{V_n})^{k_v}$, and $P_n(\frac{f}{f_n})^{k_f}$ for ZIP and EXP models. In this context, these mathematical terms could be named ZC, IC, PC, linear frequency (LF), exponential voltage (EV), and exponential frequency (EF), respectively. This terminology allows for a clear classification of the reviewed papers into these six distinct categories, as illustrated in Table 2, which provides valuable insights into the diversity of static load model considerations. It is noteworthy that in these mathematical terms, $k_v$ and $k_f$ are parameters related to voltage and frequency terms, respectively.

In this paper, since the aim is to investigate the frequency behavior of the system in the presence of different load models, the mathematical terms of LF and EF are of interest. To accomplish this, a ZIP load model represented by Equation (1), as described in reference [21], is examined to assess the impact of the LF term on the system's frequency response. Additionally, an EXP load model is considered as in [8], with a particular emphasis on the EF term, detailed in Equation 2. It is noteworthy that in the systems with approximately constant voltage profile, which could achieved by various voltage regulation methods (such as [31], [32], [33], and [34]), the voltage term could be ignored in the considered equations for ZIP and EXP models.

$$P_{ZIP} = P_n(1 + k_{ZIP}\Delta f) \tag{1}$$

$$P_{EXP} = P_n\left(\frac{f}{f_n}\right)^{k_{EXP}} \tag{2}$$

### B. DYNAMIC LOAD MODELS

In spite of static load models, dynamic models take the response time of loads into account. The most well-known dynamic load is the induction motor which is a huge proportion of the industrial load. There are various representations for IM modeling in the literature from first-order model in [35] to third- and fifth-order models in [36] and [37], respectively. The model order refers to the share of static loads as well as dynamic loads in the mixture of the load model [8].

In this paper, the considered model for induction motor, in order to study its effect on the frequency response of the system, is the fourth-order state-space model represented by [38] and [39]. In this regard, the following equations have been cisonsidered in order to model squirrel-cage IM loads.

$$V_{qs} = R_s i_{qs} + \frac{d\phi_{qs}}{dt} + \omega\phi_{ds} \tag{3}$$

$$V_{ds} = R_s i_{ds} + \frac{d\phi_{ds}}{dt} - \omega\phi_{qs} \tag{4}$$

$$V'_{qr} = R'_r i'_{qr} + \frac{d\phi'_{qr}}{dt} + (\omega - \omega_r)\phi'_{dr} \tag{5}$$

$$V'_{dr} = R'_r i'_{dr} + \frac{d\phi'_{dr}}{dt} - (\omega - \omega_r)\phi'_{qr} \tag{6}$$

$$T_e = 1.5p\left(\phi_{ds} i_{qs} - \phi_{qs} i_{ds}\right) \tag{7}$$

$$\phi_{qs} = L_s i_{qs} + L_m i'_{qr} \tag{8}$$

$$\phi_{ds} = L_s i_{ds} + L_m i'_{dr} \tag{9}$$

$$\phi'_{qr} = L'_r i'_{qr} + L_m i_{qs} \tag{10}$$

$$\phi'_{dr} = L'_r i'_{dr} + L_m i_{ds} \tag{11}$$

$$L_s = L_{ls} + L_m \tag{12}$$

$$L'_r = L'_{lr} + L_m \tag{13}$$

Also, the following two equations have been considered as the mechanical system of the IM model.

$$\frac{d}{dt}\omega_m = \frac{1}{2H}(T_e - F\omega_m - T_m) \tag{14}$$

$$\frac{d}{dt}\theta_m = \omega_m \tag{15}$$

Equations (3) to (15) depict the behavior of IMs within power systems. However, according to [18], IMs can be associated with three categories of mechanical loads, as indicated by the following equations. In this context, Equation (16) indicates the mechanical loads with constant torque and Equation (17) is responsible to the mechanical loads that their torque changes linearly with respect to the shaft speed of the IM. Also, Equation (18) represents the quadratic mechanical loads. The mechanical loads presented in Equations (16) to (18) are named as type A, B, and C, respectively in this paper. Additionally, for a better illustration, the torque-speed curves for all three types of mechanical loads are demonstrated in Fig.1.

$$T_{m,a} = T_a \tag{16}$$

$$T_{m,b} = T_b\omega_m \tag{17}$$

$$T_{m,c} = T_c\omega_m^2 \tag{18}$$

In Equations (16) to (18), $T_a$, $T_b$, $T_c$ are constant parameters and $T_{m,a}$, $T_{m,b}$, $T_{m,c}$ demonstrate the torque of different mechanical loads.

Other than IMs, there is another type of dynamic load model suggested by [4] by the name of time-delayed (TD) load. In this model, which aims to show the dynamic behavior of delayed loads, the load power consumption change is proportional to the change in frequency with a delay. Therefore, in this model, as Equation (19) indicates,

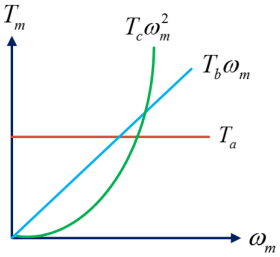


**FIGURE 1.** Torque-speed curves of mechanical load types.

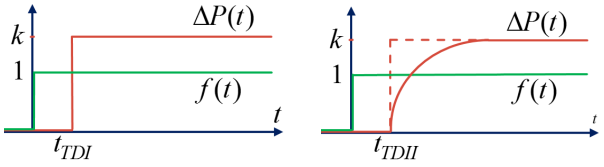


(a) TDI model (b) TDII model

**FIGURE 2.** Load change when frequency change is a unit step for TDI and TDII models.

the load power is not only a function of frequency changes but also a function of time. For a better illustration, the $\Delta f(t)$ and $\Delta P(t)$ in the case that the frequency change is a unit step function (i.e., $\Delta f(t) = u(t)$) are shown in Fig.2 (a). According to the figure, the load power follows the frequency change after a delay of $t_{TDI}$. It is noteworthy that because two TD load models are introduced in this paper, the time-delayed loads are named as TDI (type one) and TDII (type two) in the rest of the paper. Hence, the time-delayed load model of reference [4] is named TDI.

$$\Delta P_{TDI}(t) = k_{TDI}\,\Delta f(t - t_{TDI}) \tag{19}$$

In this paper, to complete the TDI model presented in Equation (19), a time constant (i.e., $\tau_{TDII}$) is introduced into the equation, which transforms Equation (19) into Equation (20). The new devised model is named time-delayed load model type two (i.e., TDII) in this study. Similar to the TDI model, the response of TDII model to a unit step function (i.e., $\Delta f(t) = u(t)$) will be equal to $\Delta P(t)$ which is demonstrated along with the $\Delta f(t)$ signal in Fig.2 (b).

$$\Delta P_{TDII}(t) = k_{TDII}\, e^{\frac{-(t-t_{TDII})}{\tau_{TDII}}}\, \Delta f(t - t_{TDII}) \tag{20}$$

Following the introduction of TDI and TDII, all load models influenced by the system's frequency could be represented through the set of $\{PC, ZIP, EXP, IM, TDI, TDII\}$. In this paper, these loads are collectively referred to as Frequency-Dependent Models (FDMs). In this regard, the effects of all six FDMs on the frequency response of the power system are investigated in the rest of this paper. It is noteworthy that the PC load is a specialization of ZIP and EXP loads and is used as a baseline for comparing the effect of load types.

## III. FREQUENCY RESPONSE METRICS

In the power systems, whenever a change happens in the total load amount or in the total generation amount,

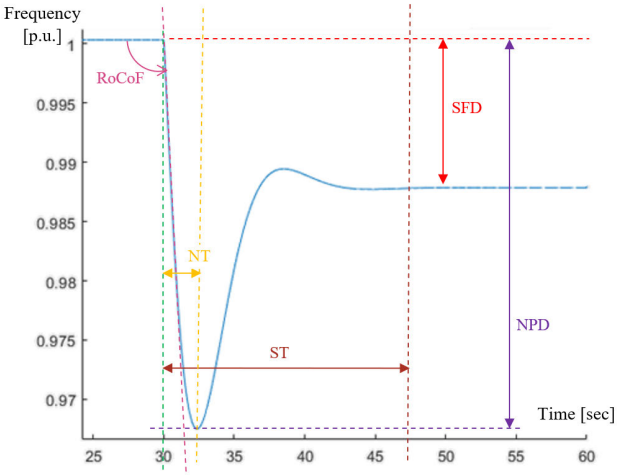


**FIGURE 3.** An idealized frequency response to a change in load/generation.

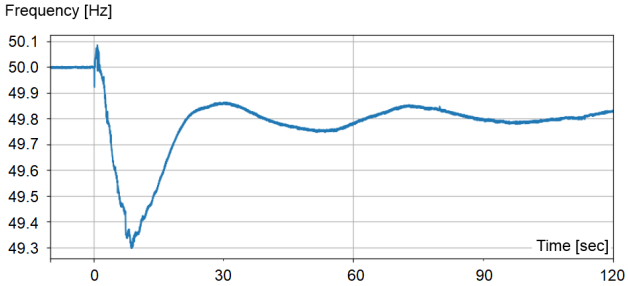


**FIGURE 4.** A real example of frequency response to disturbances in the system [40].

a frequency change occurs as depicted in Fig.3. In this regard, in order to study the frequency response of the power system, five metrics are taken into account in this paper to describe the response. The considered metrics include settling frequency deviation (SFD), rate of change of frequency (RoCoF), nadir point deviation (NPD), settling time (ST), and nadir time (NT), which are elaborated on in the following subsections. These metrics are depicted in Fig.3, showcasing an idealized frequency event response of the system. It's worth noting that a real frequency response example to a major disturbance within power systems is illustrated in Fig.4. In this event, a severe disturbance of missing more than $2000MW$ of generation within the Nordic power system happens at $6:40AM$ on April $26^{th}$, according to a report presented by Svenska Kraftnät company [40]. In Fig.4, in the beginning of the disturbance, an enter area oscillation between the generator groups can be seen. The slower oscillation in the latter part of the signal is due to the turbine governors. Here, all the generators oscillate in the same pace. Nevertheless, in this paper, for a more precise and comprehensive analysis of frequency response, the disturbance happening in the system is assumed to be only one load switching. Hence, an idealized frequency response is considered to the mentioned frequency event as depicted in Fig.3.

### A. SETTLING FREQUENCY DEVIATION (SFD)

In this paper, settling frequency deviation (SFD) metric is defined as the difference between the settling frequency and the steady state value of frequency before the event [8]. The settling frequency represents the point at which the frequency stabilizes following an event. In this regard, a higher SFD suggests that additional actions may be required from the operator to facilitate a complete recovery of the frequency [5].

### B. RATE OF CHANGE OF FREQUENCY (ROCOF)

The RoCoF metric illustrates how quickly the system's frequency changes in response to a frequency event, as depicted in Fig.3. In this context, the RoCoF of the frequency response is calculated using the following equation in this paper [25], considering the fact that the frequency event takes place at $t = 30sec$

$$RoCoF = \frac{\Delta f}{\Delta t} = \frac{f(t = 31.5) - f(t = 30)}{1.5} \tag{21}$$

### C. NADIR POINT DEVIATION (NPD)

This metric measures the difference between the nadir point of the frequency response signal and the steady frequency before the event [8]. The nadir point of the signal is defined as the minimum point in the signal after the occurrence of an event.

### D. SETTLING TIME (ST)

After the occurrence of a frequency event in the power system, the system's frequency changes. The time it takes for the frequency to reach a steady state value is called settling time [5]. To be more specific, here, the settling time is defined as the time that frequency value reaches $\eta$ percent of its steady state value (i.e., $f_{ss}$ ), starting from the event instant. This statement could be expressed mathematically in Equation (22).

### E. NADIR TIME (NT)

$$ST = Min x | \forall t \geq x, |f(t) - f_{ss}| < (1 - \eta) f_{ss} \tag{22}$$

The final metric introduced in this paper is the nadir time (NT) signifying the duration from the moment of the event to the occurrence of the nadir point in the frequency response [5].

## IV. CASE STUDY

In this section, the simulation results conducted within this study are presented and analyzed. Specifically, the IEEE 30-bus test system (which is shown in Fig.5.) is employed and implemented within MATLAB's Simulink environment. The power system configuration comprises two synchronous generators, with a 200 MW generator linked to the first bus and a 100 MW generator linked to the second bus. In this paper, in order to simulate a low inertia power system and to highlight the effects of loads, the generators' inertia constants are considered to be two seconds. Initially, a baseline case is assumed in which all of the loads are PC type in the system. The amount of PC load in each bus of the system in the baseline case is presented in Table 3. According to the table, there is 275MW PC load connected to the network in total. In order to simulate a load change in the power system and study the frequency response, a 50 MW PC load gets connected to bus 22 at $t = 30sec$ in the simulation. The simulation is run for 60 seconds, and the frequency of the system is measured on bus 19 (which has been selected randomly) to analyze the frequency response. This baseline case is used in all the studies and results in the rest of this paper for the sake of comparison. It is noteworthy that in this paper, for obtaining ST metric, $f_{ss}$ is assumed to be equal to the value of the frequency at $t = 60sec$, and the $\eta$ is presumed to be 99.998%.

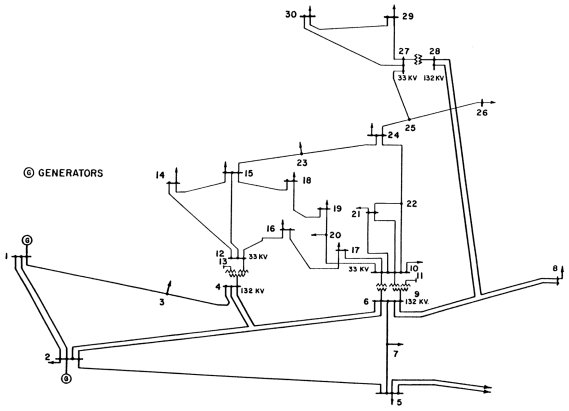


**FIGURE 5.** The one-line diagram of the IEEE 30-bus test system [41].

**TABLE 3.** Baseline load data of the test system.

| Bus | Load (MW) | Bus | Load (MW) | Bus | Load (MW) |
|---|---|---|---|---|---|
| 1 | 0 | 11 | 0 | 21 | 17.5 |
| 2 | 22.7 | 12 | 11.2 | 22 | 0 |
| 3 | 2.4 | 13 | 0 | 23 | 3.2 |
| 4 | 58.2 | 14 | 6.2 | 24 | 8.7 |
| 5 | 34.2 | 15 | 8.2 | 25 | 0 |
| 6 | 0 | 16 | 3.5 | 26 | 3.5 |
| 7 | 22.8 | 17 | 9 | 27 | 0 |
| 8 | 30 | 18 | 3.2 | 28 | 0 |
| 9 | 0 | 19 | 9.5 | 29 | 2.4 |
| 10 | 5.8 | 20 | 2.2 | 30 | 10.6 |

In the rest of this section, three different studies have been conducted. First, the effect of FDMs' parameters on the frequency response of the system are investigated. Second, the effect of their penetration level (PL) on the frequency response is studied. In this paper, penetration level of a load type is defined as the proportion of its power amount to the total load amount of the system. Finally, in the third case study, the influence of IMs' different mechanical load types on the frequency response of the system is surveyed.

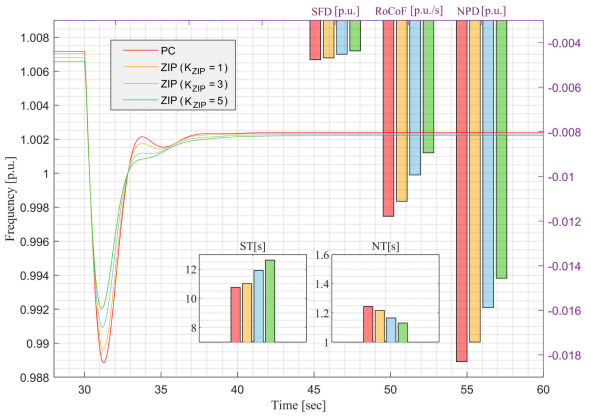


**FIGURE 6.** Frequency responses and their calculated metrics for various largeness parameter values of ZIP loads.

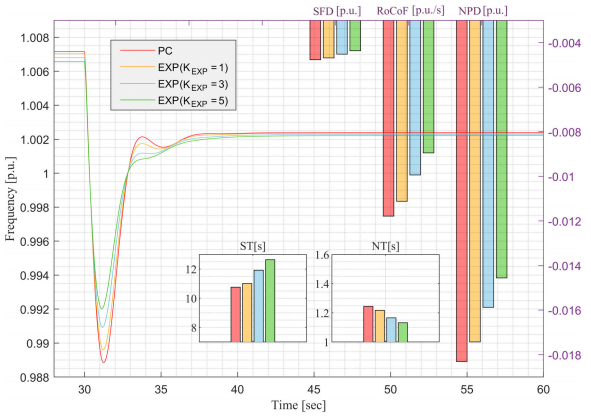


**FIGURE 7.** Frequency responses and their calculated metrics for various largeness parameter values of EXP loads.

### A. INVESTIGATIONS ON THE EFFECT OF FDMS' PARAMETERS ON FREQUENCY

In this subsection, the aim is to study the impact of each FDM on the frequency of the power system. To this end, six examination scenarios are considered to survey. In this regard, in the first scenario, four cases are considered, the first one of which is the aforementioned baseline case. To build the other three cases, 50% of PC loads in every bus in the baseline case is replaced by the ZIP load with the $k_{ZIP}$ parameter of 1, 3, and 5 in each case. In all of the four cases, an extra 50MW PC load is connected through a switch at $t = 30sec$ to bus 22, and the simulation is run for 60 seconds. The frequency response of the system (which is measured on bus 19) in each case of the first scenario is illustrated in Fig.6. According to the figure, as the ZIP load parameter (i.e., $k_{ZIP}$) increases, the SFD, RoCoF, NPD, and NT metrics of the frequency response diminish, but ST of the response increases.

To build the other scenarios for the investigation of FDMs, the ZIP loads in scenario 1 is replaced by EXP loads, IM loads, TDI loads, and TDII loads to represent scenarios 2, 3, 4, and 5, respectively. In this context, in scenario 2, the EXP load parameter (i.e., $k_{EXP}$) is set to 1, 3, and 5 to investigate its effect on the frequency. In scenario 3, the inertia of all the IMs is set to 1, 2, and 3 seconds in each case to survey the influence of inertia on the system's frequency. Afterward, scenario 4 takes the *TDI* load into the account with parameter $t_{TDI}$ equal to 0.1, 0.5, and 0.9 seconds for each case. Finally, in scenario 5, $\tau_{TDII}$ is similarly set to 0.1, 0.5, and 0.9 seconds for each case to survey its effect on the frequency. It is noteworthy that the mechanical load type for all IMs in scenario 3 is considered to be the mechanical load type A with $T_a = 1$ for all cases. Also, in scenarios 4 and 5, $k_{TDI} = k_{TDII} = 2$ is kept constant in all cases, and $t_{TDII}$ is kept fixed to be equal to zero in scenario 5. In other words, scenario 4 aims to study the effect of $t_{TDI}$ while scenario 5 investigates only the effect of $\tau_{TDII}$ parameter.

The results of simulations for scenarios 2 to 5 is presented within the Figures 7 to 10, respectively. In this regard, according to Fig.7, similar to the effect of $k_{ZIP}$, with the increment of $k_{EXP}$, the SFD, RoCoF, NPD, and NT metrics of

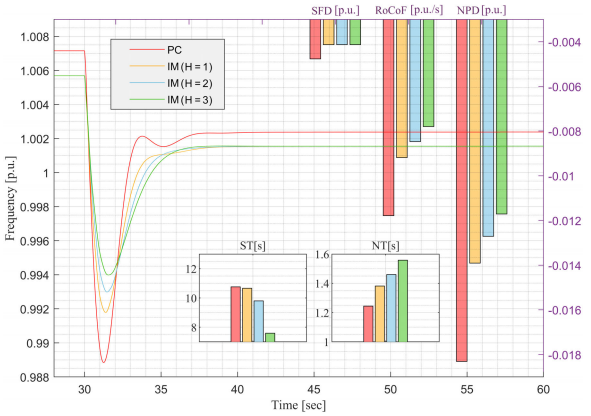


**FIGURE 8.** Frequency responses and their calculated metrics for various inertia values of IM loads.

the frequency response decrease; however, the ST increases. Hence, the frequency response for both ZIP and EXP loads are quite similar so that it can be concluded ZIP model is an approximate for EXP model when frequency change is small.

Thereafter, the results of scenario 3, in which the IM load behavior is investigated, are demonstrated in Fig.8. According to the results, by the increment of IMs' inertia, the RoCoF, ND, and ST metrics of the frequency response decrease. The SFD of the frequency response diminishes when the IM load is added to the system, but by the increment of IMs inertia, it does not change. Therefore, overall, it is seen that IM loads improve the frequency response of the system by shifting the nadir point upward and diminishing the RoCoF.

After conducting investigations on the impact of IMs, scenarios 4 and 5 were designed to analyze the influence of TDI and TDII loads, respectively. As demonstrated in Figures 9 and 10, the introduction of TDI and TDII loads into the system raises the nadir point since it amplifies loads' dependency on frequency. Therefore, in the transition from case 1 to case 2, the RoCoF and NPD of the response decrease. However, with an increase in the values of parameters $t_{TDI}$ and $\tau_{TDII}$, the loads' dependency on frequency diminishes due to an extended delay compared to before, resulting in an increase in RoCoF and NPD.

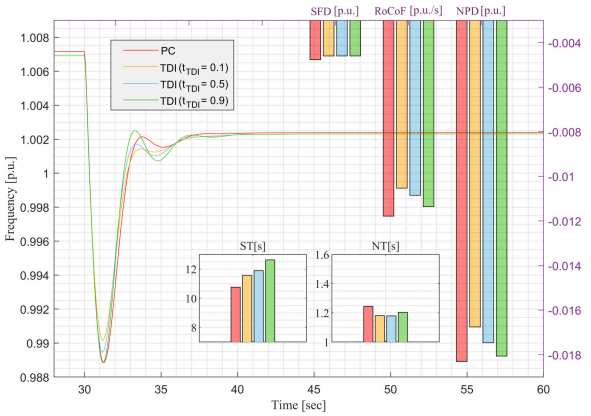


**FIGURE 9.** Frequency responses and their calculated metrics for various delay times of TDI loads.

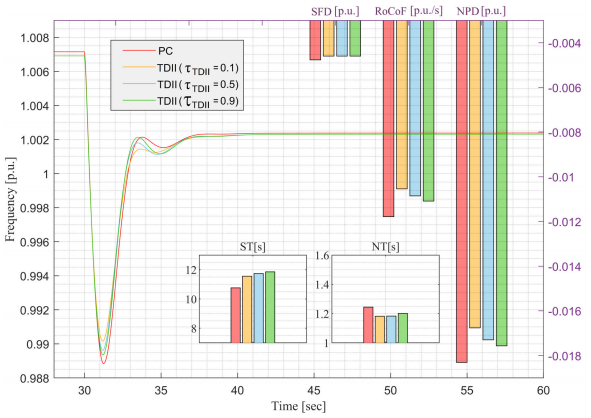


**FIGURE 10.** Frequency responses and their calculated metrics for various time constants of TDII loads.

Additionally, the SFD and NT of the response decrease when TDI and TDII loads are integrated into the system. These metrics, however, remain relatively stable despite increments in the $t_{TDI}$ and $\tau_{TDII}$ parameters. Nevertheless, as TDI and TDII loads introduce more transient overshoots into the response, the ST metric increases. In summary, it could be concluded that TDI and TDII loads affect the frequency of the system adversely as the values of $t_{TDI}$ or $\tau_{TDII}$ increase.

Lastly, the sixth scenario encapsulates the comprehensive view of all FDMs in a single context. This scenario encompasses a total of six cases in which the initial case is the previously mentioned baseline case. To configure the remaining five cases, half of the loads at each bus is replaced with ZIP, EXP, IM, TDI, and TDII loads, corresponding to the construction of cases 2 through 6, respectively. In these cases, the parameters of loads are considered as the following values. It is noteworthy that the mechanical load of IMs is considered to be type A in this scenario.

$$k_{ZIP} = k_{EXP} = k_{TDI} = k_{TDII} = 2$$
$$t_{TDI} = \tau_{TDII} = 0.5sec, t_{TDII} = 0sec$$
$$H = 2sec, T_a = 1\ p.u.$$

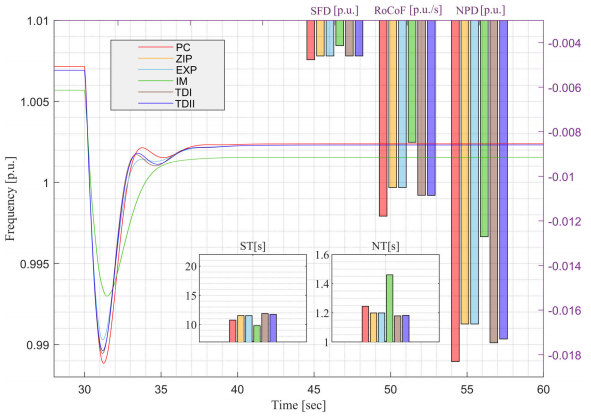


**FIGURE 11.** Frequency responses and their calculated metrics when 50% of PC loads are replaced by each load type.

According to Fig.11, which is responsible for the results of scenario 6, IMs have the most effect on decrement of SFD, RoCoF, NPD, and ST metrics. However, they cause the frequency response to have more NT in comparison with other loads. Moreover, ZIP and EXP loads lower the SFD, RoCoF, NPD, and NT metrics of the frequency response compared to the baseline case, but they enhance the ST metric. The effect of TDI and TDII loads are similar to the ZIP and EXP loads, but with less changes in the RoCoF and NPD as well as more changes in the ST and NT. However, the effect of TDI and TDII loads, as seen previously, is highly dependent on their parameters (i.e., $t_{TDI}$, $t_{TDII}$, or $\tau_{TDII}$).

### B. INVESTIGATIONS ON THE EFFECT OF FDMS' PL ON FREQUENCY

Following the examination of how FDM loads impact the system's frequency response, this subsection delves into the exploration of the impact of PL of the FDM loads. To this end, five scenarios have been considered involving ZIP, EXP, IM, TDI, and TDII loads. Each scenario encompasses four cases: the first case represents the baseline scenario, the second case incorporates a PL of 20%, the third case increases the PL to 40%, and the final case raises the PL to 60%.

In this regard, the results of the scenarios 1 to 5 are represented in Figures 12 to 16, respectively. As indicated in these figures, by increasing the total amount of FDM, the nadir point of the frequency response is shifted upward. Therefore, the NPD of the response, as well as the RoCoF metric, decreases. Also, because the FDM loads increase, more percentage of the system load gets dependent on the frequency of the system. As a result, the SFD of the frequency response also decreases in the mentioned figures.

Additionally, according to Figures 12, 13, 15 and 16, when the PLs of ZIP, EXP, TDI, and TDII loads increase, the ST of their corresponding frequency response increases while the NT metric decreases. This is because of the nature of the load types and could be seen in the transition from case 1 to 2 (when the FDM loads get connected to the system) in Figures 6, 7, 9 and 10. However, according to Fig.14., by enhancing the PL of IMs, the ST of the response decreases

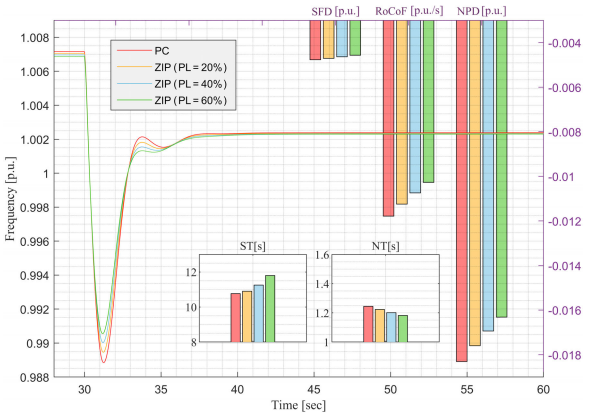


**FIGURE 12.** Frequency responses and their calculated metrics for different ZIP load PLs.

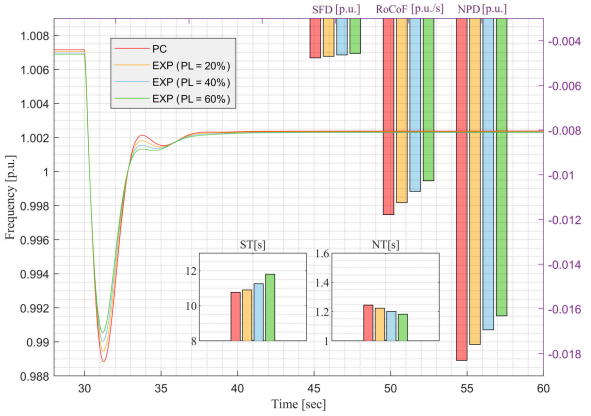


**FIGURE 13.** Frequency responses and their calculated metrics for different EXP load PLs.

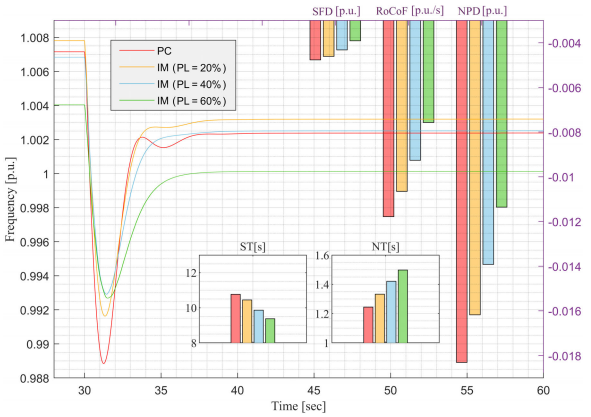


**FIGURE 14.** Frequency responses and their calculated metrics for different IM load PLs.

and the NT increases. These trends of ST and NT are similar to the trends in Fig.8. indicating that the impact of IM load amount increment is similar to the enhancement in their inertia.

### C. SURVEY ON MECHANICAL LOADS OF IM

As previously outlined, IMs can be connected to three types of mechanical loads, denoted as A, B, and C, as expressed in Equations (16) to (18). In this section, a scenario is devised for the sake of exploring the impact of these various mechanical

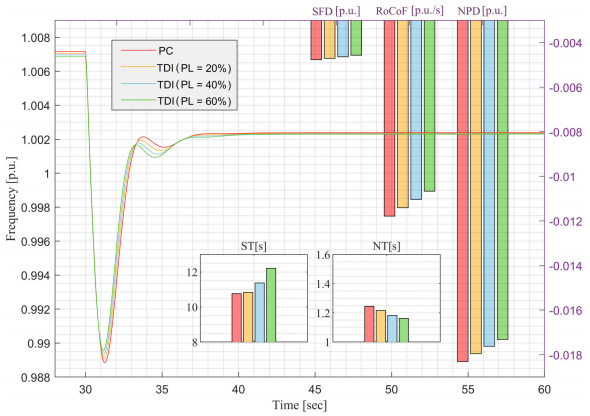


**FIGURE 15.** Frequency responses and their calculated metrics for different TDI load PLs.

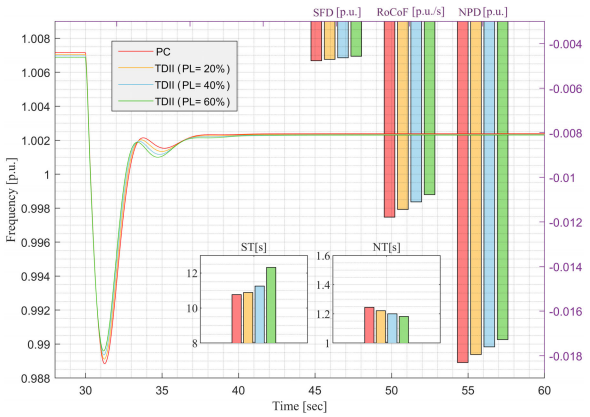


**FIGURE 16.** Frequency responses and their calculated metrics for different TDII load PLs.

loads on the system's frequency response. Within this context, four specific cases are examined. The initial case serves as the baseline scenario. In the second case, half of the loads from the baseline scenario are substituted with IMs bearing mechanical load type A. The third case involves mechanical load type B, and in the final case, mechanical load type C is applied. It is noteworthy that in all these cases, the inertia values of IMs are kept constant and equal to two seconds. Moreover, the values of $T_a$, $T_b$, and $T_c$ are assumed to be one p.u. for each IM (which is equal to the nominal power of each IM divided by the synchronous speed).

By implementation of this scenario, as shown in Fig.17, the SFD, RoCoF, and NPD of the frequency response decrease for mechanical load types A to C. This is because in transition from mechanical load type A to C, the dependency to the $\omega_m$, which is related to the frequency of the system, increases. Therefore, the dependency to the system's frequency increases, resulting in upward shift of the nadir point.

Furthermore, the ST metric in the frequency response increases, while the NT metric diminishes during the transition from mechanical load type A to C. This trend could be attributed to the upward shifting of the frequency response signal. This shift stems from the slightly reduced mechanical load power consumption of IMs as they transition from load

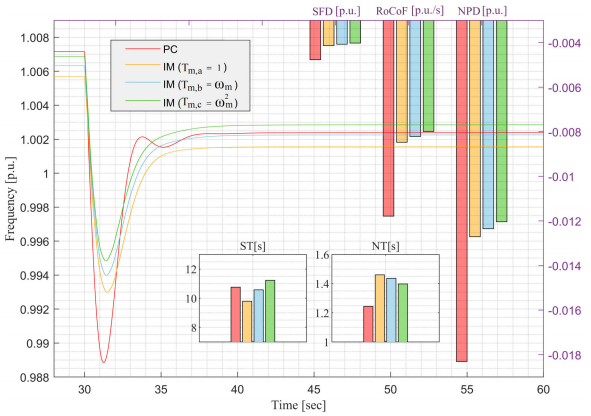


**FIGURE 17.** Frequency responses and their calculated metrics for different mechanical loads of IMs.

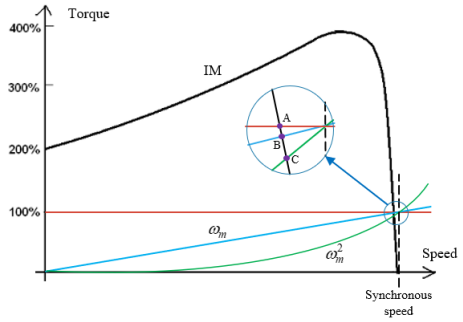


**FIGURE 18.** Operational point of IMs in different mechanical loads.

**TABLE 4.** Investigated load parameters' effect on the frequency response of the system.

| Case study section | Experiment | | Result trend in $\lvert SFD \rvert$ | $\lvert RoCoF \rvert$ | $\lvert NPD \rvert$ | $ST$ | $NT$ |
|---|---|---|---|---|---|---|---|
| A | $k_{ZIP}, k_{EXP}$ | ↑ | ↓ | ↓ | ↓ | ↑ | ↓ |
| | $H$ | ↑ | - | ↓ | ↓ | ↓ | ↑ |
| | $\tau_{TDI}, \tau_{TDII}$ | ↑ | - | ↑ | ↑ | ↑ | - |
| B | ZIP, EXP, TDI, TDII loads' PL | ↑ | ↓ | ↓ | ↓ | ↑ | ↓ |
| | IM loads' PL | ↑ | ↓ | ↓ | ↓ | ↓ | ↑ |
| C | IMs mechanical load $\omega_m$ exponent | ↑ | ↓ | ↓ | ↓ | ↑ | ↓ |

type A to C. The decrease is associated with the nominal operational point of IMs, as demonstrated in Fig.18, which slightly decreases during this transition. Consequently, the mechanical torque decreases while the shaft speed remains relatively constant, leading to a reduction in mechanical power during the shift from load type A to C.

It is noteworthy that a concise summary of the findings from this study is provided in Table 4. In this table, the effects of increasing FDMs' parameters, enhancing their PL, as well as the effect of increasing exponent of $\omega_m$ in the mechanical load of IM are represented. Notably, the symbols "↑", "↓", and "-" denote an increase, decrease, and no change, respectively, in the table.

## V. CONCLUSION

In conclusion, this study provides a comprehensive analysis of loads affecting the system's frequency. It not only introduces an enhanced model for time-delayed loads but also systematically classifies these loads. Subsequently, an in-depth exploration is undertaken to understand how different load parameters, along with their penetration levels, influence the system's frequency. To empirically investigate these effects, an IEEE 30-bus test system is selected as the experimental platform. Then, the impacts of FDMs' parameters, their PL, and the exponent of $\omega_m$ in the mechanical load of IM are investigated within the test system. Results are indicative of the pronounced impact of IM loads, which significantly shift the nadir point of the system's frequency response upward, resulting in a reduction of SFD, RoCoF, and NPD metrics. Furthermore, an increase in the presence of FDM within the power system correlates with a shifted nadir point in the frequency response and a simultaneous reduction in SFD, RoCoF, and NPD metrics. This research contributes valuable insights into the dynamics of different loads on power system frequency and offers a basis for further studies and decision-making within the energy sector.

## REFERENCES

[1] P. Sorensen, N. A. Cutululis, A. Vigueras-Rodriguez, L. E. Jensen, J. Hjerrild, M. H. Donovan, and H. Madsen, "Power fluctuations from large wind farms," *IEEE Trans. Power Syst.*, vol. 22, no. 3, pp. 958–965, Aug. 2007.

[2] N. Miller, M. Shao, S. Pajic, and R. D'Aquila, "Eastern frequency response study," Nat. Renew. Energy Lab. (NREL), Golden, CO, USA, NREL Tech. Rep. NREL/SR-5500-58077, 2013. [Online]. Available: https://www.nrel.gov/docs/fy13osti/58077.pdf

[3] J. D. R. Penaloza, J. A. Adu, A. Borghetti, F. Napolitano, F. Tossani, and C. A. Nucci, "Influence of load dynamic response on the stability of microgrids during islanding transition," *Electr. Power Syst. Res.*, vol. 190, Jan. 2021, Art. no. 106607.

[4] M. Amini and M. Almassalkhi, "Investigating delays in frequency-dependent load control," in *Proc. IEEE Innov. Smart Grid Technol.-Asia (ISGT-Asia)*, Nov. 2016, pp. 448–453.

[5] E. Polykarpou, M. Asprou, E. Kyriakides, C. Hadjilaou, A. Petoussis, and Z. Achillides, "Effect of load composition on the frequency response of the Cyprus power system," in *Proc. IEEE Int. Conf. Sci. Electr. Eng. (ICSEE)*, Dec. 2018, pp. 1–5.

[6] P. S. Kundur, "Power system stability," in *Power System Stability and Control*, vol. 10. Boca Raton, FL, USA: CRC Press, 2007, pp. 1–7. [Online]. Available: https://www.taylorfrancis.com/books/edit/10.4324/b12113/power-system-stability-control-leonard-grigsby?refId=1660808c-3bdb-4c50-b6e9-1e0cece0da58&context=ubx

[7] A. Arif, Z. Wang, J. Wang, B. Mather, H. Bashualdo, and D. Zhao, "Load modeling—A review," *IEEE Trans. Smart Grid*, vol. 9, no. 6, pp. 5986–5999, Nov. 2018.

[8] I. D. Pasiopoulou, E. O. Kontis, T. Papadopoulos, and G. K. Papagiannis, "Effect of load modeling on power system stability studies," *Electr. Power Syst. Res.*, vol. 207, Jun. 2022, Art. no. 107846.

[9] W. Price, S. Casper, C. Nwankpa, R. Bradish, H. Chiang, C. Concordia, J. Staron, C. Taylor, E. Vaahedi, and G. Wu, "Bibliography on load models for power flow and dynamic performance simulation," *IEEE Power Eng. Rev.*, vol. 15, no. 2, p. 70, Feb. 1995. [Online]. Available: https://www.osti.gov/biblio/49243

[10] D. del Giudice, F. Bizzarri, S. Grillo, D. Linaro, and A. M. Brambilla, "Impact of passive-Components' models on the stability assessment of inverter-dominated power grids," *Energies*, vol. 15, no. 17, p. 6348, Aug. 2022.

[11] A. S. Ahmadyar, S. Riaz, G. Verbic, A. Chapman, and D. J. Hill, "A framework for assessing renewable integration limits with respect to frequency performance," *IEEE Trans. Power Syst.*, vol. 33, no. 4, pp. 4444–4453, Jul. 2018.

[12] A. Haque and A. Bhuiya, "The role of synthetic inertia and effective load modelling in providing system stability as renewable energy penetration increases," in *Proc. IEEE Ind. Appl. Soc. Annu. Meeting*, Oct. 2020, pp. 1–6.
[13] J. Gouveia, C. L. Moreira, and J. A. P. Lopes, "Influence of load dynamics on converter-dominated isolated power systems," *Appl. Sci.*, vol. 11, no. 5, p. 2341, Mar. 2021.
[14] J. Ma, D. Han, R.-M. He, Z.-Y. Dong, and D. J. Hill, "Reducing identified parameters of measurement-based composite load model," *IEEE Trans. Power Syst.*, vol. 23, no. 1, pp. 76–83, Feb. 2008.
[15] M. J. Rainey and D. T. O. Oyedokun, "Load modelling effects on power system inertia response," in *Proc. IEEE PES/IAS PowerAfrica*, Aug. 2020, pp. 1–5.
[16] A. Bokhari, A. Alkan, R. Dogan, M. Diaz-Aguiló, F. de León, D. Czarkowski, Z. Zabar, L. Birenbaum, A. Noel, and R. E. Uosef, "Experimental determination of the ZIP coefficients for modern residential, commercial, and industrial loads," *IEEE Trans. Power Del.*, vol. 29, no. 3, pp. 1372–1381, Jun. 2014.
[17] C. Grande-Moran, B. Fernandes, D. Feltes, J. Feltes, M. Wu, and R. Wells, "Case studies on dynamic load modeling," in *Proc. Clemson Univ. Power Syst. Conf. (PSC)*, Sep. 2018, pp. 1–8.
[18] Z. Shuai, Y. Peng, X. Liu, Z. Li, J. M. Guerrero, and Z. J. Shen, "Parameter stability region analysis of islanded microgrid based on bifurcation theory," *IEEE Trans. Smart Grid*, vol. 10, no. 6, pp. 6580–6591, Nov. 2019.
[19] M. A. Rios, S. Pérez-Londoño, and A. Garcés, "Dynamic performance evaluation of the secondary control in islanded microgrids considering frequency-dependent load models," *Energies*, vol. 15, no. 11, p. 3976, May 2022.
[20] L. M. Hajagos and B. Danai, "Laboratory measurements and models of modern loads and their effect on voltage stability studies," *IEEE Trans. Power Syst.*, vol. 13, no. 2, pp. 584–592, May 1998.
[21] S. A. Saleh, J. Wo, X. F. St. Onge, and E. Castillo-Guerra, "Estimating frequency changes due to smart grid functions," in *Proc. IEEE/IAS 55th Ind. Commercial Power Syst. Tech. Conf. (I&CPS)*, May 2019, pp. 1–10.
[22] L. Zacharia, M. Asprou, E. Kyriakides, and M. Polycarpou, "Effect of dynamic load models on WAC operation and demand-side control under real-time conditions," *Int. J. Electr. Power Energy Syst.*, vol. 126, Mar. 2021, Art. no. 106589.
[23] A. Adrees and J. Milanović, "Effect of load models on angular and frequency stability of low inertia power networks," *IET Gener., Transmiss. Distribution*, vol. 13, no. 9, pp. 1520–1526, May 2019.
[24] Y. Zhu, J. V. Milanović, and K. N. Hasan, "Ranking and quantifying the effects of load model parameters on power system stability," *IET Gener., Transmiss. Distrib.*, vol. 13, no. 20, pp. 4650–4658, Oct. 2019.
[25] M. Bennett and Y. Liu, "The impact of large-scale dynamic load modeling on frequency response in the U.S. Eastern interconnection," *Int. J. Electr. Power Energy Syst.*, vol. 120, Sep. 2020, Art. no. 105983.
[26] L. Sigrist and L. Rouco, "An induction motor model for system frequency response models," *Int. Trans. Electr. Energy Syst.*, vol. 27, no. 11, p. e2413, Nov. 2017.
[27] Z. Tang, G. Mu, J. Pan, Z. Xue, H. Yang, M. Mei, Z. Zhang, and P. Kou, "Dynamic equivalent model considering multiple induction motors for system frequency response," *Energies*, vol. 16, no. 7, p. 2987, Mar. 2023.
[28] Y. Bian, H. Wyman-Pain, F. Li, R. Bhakar, S. Mishra, and N. P. Padhy, "Demand side contributions for system inertia in the GB power system," *IEEE Trans. Power Syst.*, vol. 33, no. 4, pp. 3521–3530, Jul. 2018.
[29] J. A. Short, D. G. Infield, and L. L. Freris, "Stabilization of grid frequency through dynamic demand control," *IEEE Trans. Power Syst.*, vol. 22, no. 3, pp. 1284–1293, Aug. 2007.
[30] A. Mahdavian, A. A. Ghadimi, and M. Bayat, "Microgrid small-signal stability analysis considering dynamic load model," *IET Renew. Power Gener.*, vol. 15, no. 13, pp. 2799–2813, Oct. 2021.
[31] B. A. Robbins and A. D. Domínguez-García, "Optimal reactive power dispatch for voltage regulation in unbalanced distribution systems," *IEEE Trans. Power Syst.*, vol. 31, no. 4, pp. 2903–2913, Jul. 2016.
[32] X. Hu, Z.-W. Liu, G. Wen, X. Yu, and C. Liu, "Voltage control for distribution networks via coordinated regulation of active and reactive power of DGs," *IEEE Trans. Smart Grid*, vol. 11, no. 5, pp. 4017–4031, Sep. 2020.
[33] D. Stanelyte and V. Radziukynas, "Review of voltage and reactive power control algorithms in electrical distribution networks," *Energies*, vol. 13, no. 1, p. 58, Dec. 2019.
[34] M. Tofighi-Milani, S. Fattaheian-Dehkordi, M. Fotuhi-Firuzabad, and M. Lehtonen, "Distributed reactive power management in multi-agent energy systems considering voltage profile improvement," *IET Gener., Transmiss. Distrib.*, vol. 17, no. 21, pp. 4891–4906, Nov. 2023.
[35] B.-K. Choi, H.-D. Chiang, Y. Li, H. Li, Y.-T. Chen, D.-H. Huang, and M. G. Lauby, "Measurement-based dynamic load models: Derivation, comparison, and validation," *IEEE Trans. Power Syst.*, vol. 21, no. 3, pp. 1276–1283, Aug. 2006.
[36] B. C. Lesieutre, P. W. Sauer, and A. Pai, "Development and comparative study of induction machine based dynamic P, Q load models," *IEEE Trans. Power Syst.*, vol. 10, no. 1, pp. 182–191, Feb. 1995.
[37] T. Thiringer and J. Luomi, "Comparison of reduced-order dynamic models of induction machines," *IEEE Trans. Power Syst.*, vol. 16, no. 1, pp. 119–126, Feb. 2001.
[38] N. Mohan, T. M. Undeland, and W. P. Robbins, *Power Electronics: Converters, Applications, and Design*. Hoboken, NJ, USA: Wiley, 2003.
[39] P. C. Krause, O. Wasynczuk, S. D. Sudhoff, and S. Pekarek, *Analysis of Electric Machinery and Drive Systems*, vol. 2. Hoboken, NJ, USA: Wiley, 2002.
[40] S. Kraftnät, "Driftstörningen den 26 April 2023, beskrivning av störningens händelseförlopp," Svenska Kraftnät, Stockholm, Sweden, Tech. Rep. Svk 2023/1561, 2023.
[41] M. Shahidehpour and Y. Wang, *Communication and Control in Electric Power Systems: Applications of Parallel and Distributed Processing*. Hoboken, NJ, USA: Wiley, 2004.

**MAHYAR TOFIGHI-MILANI** received the B.Sc. degree in electrical engineering from Iran University of Science and Technology (IUST), in 2018, and the M.Sc. degree in electrical engineering from the Sharif University of Technology, in 2021. He is currently pursuing the Ph.D. degree with the Electrical Engineering and Automation School, Aalto University. His research interests include smart grids, electricity markets, renewable and distributed energy resources, and microgrids.

**SAJJAD FATTAHEIAN-DEHKORDI** (Graduate Student Member, IEEE) received the M.Sc. degree in electrical engineering and power systems from the Sharif University of Technology, Tehran, Iran, in 2014, and the joint Ph.D. degree from the Sharif University of Technology and Aalto University, Espoo, Finland, in 2023. His research interests include power systems planning, operations, and economics, with a focus on issues relating to the integration of renewable energy resources into the systems.

**MATTI LEHTONEN** received the master's and Licentiate degrees in electrical engineering from Helsinki University of Technology, in 1984 and 1989, respectively, and the Doctor of Technology degree from Tampere University of Technology, in 1992. He has been a Professor with Helsinki University of Technology (now Aalto University), where he is currently the Head of the Power Systems and High Voltage Engineering Laboratory. His research interests include power system planning and asset management and power system protection, including earth fault problems, harmonic related issues, and applications of information technology in distribution systems.